Macromolecules

Article

pubs.acs.org/Macromolecules

Complementary Semiconducting Polymer Blends: Influence of Side Chains of Matrix Polymers

Xikang Zhao,[†] Guobiao Xue,[†,§] Ge Qu,[∥] Vani Singhania,[†] Yan Zhao,[†] Kamal Butrouna,[⊥] Aristide Gumyusenge,[†] Ying Diao,[∥] Kenneth R. Graham,[⊥] Hanying Li,[§] and Jianguo Mei*[,†,‡]

[†]Department of Chemistry and [‡]Birck Nanotechnology Center, Purdue University, West Lafayette, Indiana 47907, United States

[§]MOE Key Laboratory of Macromolecule Synthesis and Functionalization, State Key Laboratory of Silicon Materials, Department of Polymer Science and Engineering, Zhejiang University, Hangzhou 310027, P. R. China

[∥]Department of Chemical & Biomolecular Engineering, University of Illinois at Urbana−Champaign, Urbana, Illinois 61801, United States

[⊥]Department of Chemistry, University of Kentucky, Lexington, Kentucky 40506, United States

Supporting Information

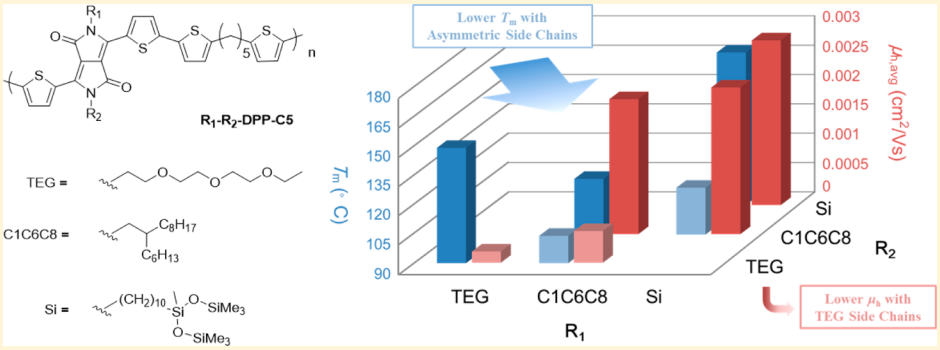

ABSTRACT: The concept of complementary semiconducting polymer blends (*c*-SPBs) has been recently proposed to achieve enhanced solution processability and/or melt-processing capability for organic electronics. In the previous study, we demonstrated the impact of conjugation-break spacers of matrix polymers. In the current work, we explore the influence of the side chains of the matrix polymer on the physical properties of the pure polymers and their corresponding *c*-SPBs, including electrical properties and phase transition behaviors. Six diketopyrrolopyrrole (DPP)-based polymers with pentamethylene conjugation-break spacers (CBSs) and various side chains, including branched-alkyl, triethylene glycol (TEG), and siloxane-terminated side chains, were synthesized and characterized. The UV−vis spectra show that the side chains have a noticeable impact on the intermolecular interactions in the solid states. In addition, side chains also have a significant influence on the thermal behaviors of the polymers. Polymers with asymmetric side chains attached to the same DPP unit exhibit lower melting points compared to the congeners with symmetric side chains. The polymer with both branched-alkyl and TEG side chain exhibits the lowest melting point of 104 °C. As for charge transport properties, polymers with branched-alkyl and/or siloxane-terminated side chains give hole mobilities on the same order of magnitude, whereas the polymers with TEG side chains exhibits much lower mobilities. When *c*-SPBs with a fully conjugated polymer with branched-alkyl side chains are concerned, the *c*-SPBs of all polymers, except for the polymer with only TEG side chains (TEG-DPP-C5), show hole mobilities 2 orders of magnitude higher than the corresponding pure matrix polymers. In contrast, TEG-DPP-C5 merely presents an improvement of 20 times, which resulted from the incompatibility of TEG side chains from the matrix polymer and the alkyl side chains from the tie chain polymer. These results provide new insights into structural design for semiconducting materials with both high performance and better processability.

INTRODUCTION

Materials design, processing, and device fabrication are contributing to the harvest of semiconducting polymers' performance. Among materials design, side chain engineering serves as a crucial strategy to tune the intermolecular interactions and affect both physical and electrical properties of the materials.[1,2] For example, Feng et al. reported a series of discotics with alkyl and oligoether side chains. The drastic difference between the polarities of the side chains brought about nicely controlled molecular packing and charge carrier mobilities.[3] As for conjugated polymers, Kanimozhi et al. reported an alternating copolymer of two diketopyrrolopyrrole

Received: June 26, 2017
Revised: July 21, 2017
Published: August 10, 2017

DOI: 10.1021/acs.macromol.7b01354
Macromolecules 2017, 50, 6202−6209

Scheme 1. Syntheses and Nomenclatures for the DPP-Based Matrix Polymers with Different Side Chains

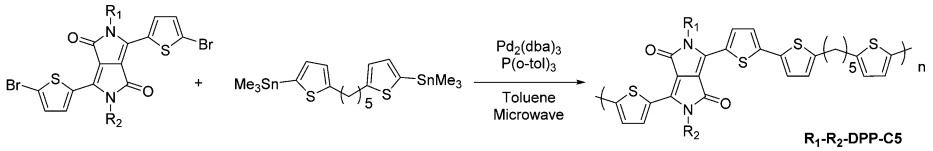

Polymer	R_1	R_2
C1C6C8-DPP-C5	C_8H_{17} / C_6H_{13}	C_8H_{17} / C_6H_{13}
C3C10C10-DPP-C5	$C_{10}H_{21}$ / $C_{10}H_{21}$	$C_{10}H_{21}$ / $C_{10}H_{21}$
TEG-DPP-C5	O_3	O_3
Si-DPP-C5	$(CH_2)_{10}$-Si(OSiMe$_3$)$_2$(OSiMe$_3$)	$(CH_2)_{10}$-Si(OSiMe$_3$)$_2$(OSiMe$_3$)
C1C6C8-TEG-DPP-C5	C_8H_{17} / C_6H_{13}	O_3
Si-C1C6C8-DPP-C5	$(CH_2)_{10}$-Si(OSiMe$_3$)$_2$(OSiMe$_3$)	C_8H_{17} / C_6H_{13}

(DPP) monomers with either alkyl or oligoether side chains. The special architecture resulted in a high electron mobility of 3 cm^2V^{-1} s^{-1}.[4] Mei et al. introduced siloxane-terminated solubilizing groups, which led to smaller $\pi-\pi$ stacking distances between polymer molecules and the presence of both face-on and edge-on orientation of the polymer molecules. These unique features of the materials favored charge transport and resulted in improved average charge carrier mobilities as high as 4.5 cm^2 V^{-1} s^{-1}.[5]

Processing practicability is another factor for the wide application of polymers. Currently, semiconducting polymers with high performance, which usually consist of fully conjugated backbones, suffer from poor solubility or high melt transition temperatures (higher than the thermal decomposition temperatures), which makes it difficult to implement industrial processing methods such as roll-to-roll processing.[6] Side chain engineering has been successful in making solution-processable materials, but the use of toxic chlorinated solvents bring about environmental and health concerns, and the existence of solvent residuals has also shown significant impacts on the performance of the materials.[7] One possible strategy to improve processability is to introduce flexible and conjugation-break spacers (CBSs) to the polymer backbones.[8−13] We recently proposed the concept of complementary semiconducting blends (*c*-SPBs). These binary systems, which are composed of fully conjugated tie-chain polymers and CBS-containing matrix polymers, showed enhanced charge carrier properties, improved solubility, and capability for melt-processing. For example, studies over the binary system with DPP-C3 as the matrix polymer and DPP-C0 as the tie-chain polymer reviewed that by adding only 1 wt % of the tie-chain polymer into the matrix polymer, the charge carrier mobility improved drastically by 2 orders of magnitude.[14] In addition, the melting point of the matrix polymer was tunable based on the length of the CBS,[15] which makes it possible to fabricate polymer-based devices without using carcinogenic chlorine-containing solvents.[16] We have revealed that the high performance of the *c*-SPBs is a result of the combination of the highly ordered $\pi-\pi$ stacking within the crystalline domains of the matrix polymers and the efficient intrachain charge transport network from the tie-chain polymer. However, how the intermolecular interactions between the two polymers influence the charge transport remains elusive.

In this study, we aim to reveal the influence of the side chains on the matrix polymers and the corresponding *c*-SPBs. From the perspective of material design, our interest lies mainly in two dimensions: charge transport properties and melt processability. DPP-based CBS polymers with different side chains were synthesized and characterized, including four with symmetric side chains (including branched-alkyl chains, oligoether chains, and siloxane-terminated side chains) on the same DPP unit and two with asymmetric side chains. The results show that charge transport properties and phase transition behaviors of the polymers exhibit strong correlation with side chains. For the charge transport properties, polymers with alkyl chains and siloxane-terminated side chains give hole mobilities on the same order magnitude, whereas the presence of polyether side chains leads to significantly lower numbers. The hole mobilities of all the *c*-SPBs are almost 2 orders of magnitude higher than that of the pure ones, except for the polymer with only oligoether side chains. As for phase transition properties, lower melting temperatures and heats of fusions are generally observed for asymmetric polymers. Grazing incidence X-ray diffraction (GIXRD) results show that the difference between the crystallinities of the pure matrix polymer and the *c*-SPBs is also dependent to the side chains. For matrix polymers with only nonpolar side chains, the crystallinity decreases with the addition of the tie chain polymer, whereas for polymers with highly polar oligoether side chains, the crystallinity increases, which indicates that side chains have a massive impact on the interaction between the matrix and tie chain polymers and thus influence the charge transport properties of the *c*-SPBs. This work also provides us with a new approach to tune melt-processability for semiconducting polymers.

DOI: 10.1021/acs.macromol.7b01354
Macromolecules 2017, 50, 6202−6209

Table 1. Physical Properties of the Matrix Polymers

	M_n (kDa)/$Đ$[a]	T_d[b] (°C)	T_m[c] (°C)	ΔH_{fus}[d] (kJ/mol)	λ_{max}^{abs} (nm) solution[e]	λ_{max}^{abs} (nm) film[f]	E_g^{opt}[g] (eV)	energy levels (eV) E_{HOMO}[h]	energy levels (eV) E_{LUMO}[i]
C1C6C8-DPP-C5	14.0/1.7	409	118	4.0	589, 624	597, 655	1.42	−5.21	−3.79
C3C10C10-DPP-C5[15]	12.9/1.3	393	138	7.3	594, 631	605, 654	1.41	−5.14	−3.75
TEG-DPP-C5	2.4/1.2	399	149	2.8	588	618	1.35	−4.99	−3.64
C1C6C8-TEG-DPP-C5	6.3/1.2	404	104	2.6	588	605	1.41	−5.13	−3.72
Si-DPP-C5	15.2/1.3	405	168	10.9	591, 625	603	1.39	−5.16	−3.77
Si-C1C6C8-DPP-C5	9.5/1.3	411	114	4.7	590, 625	605, 626	1.38	−5.19	−3.81

[a]Tetrahydrofuran as the eluent at room temperature. [b]Decomposition temperature. [c]Melting temperature. [d]Enthalpy of fusion, calculated based on repeating unit. [e]In chloroform solution. [f]Drop-casted films on glass substrates, annealed at 120 °C. [g]Calculated from the onset absorption $E_g^{opt} = 1240/\lambda_{onset}^{abs}$ (nm). [h]Obtained from UPS, uncertainty ±0.05 eV. [i]Calculated using the equation $E_{LUMO} = E_{HOMO} + E_g^{opt}$.

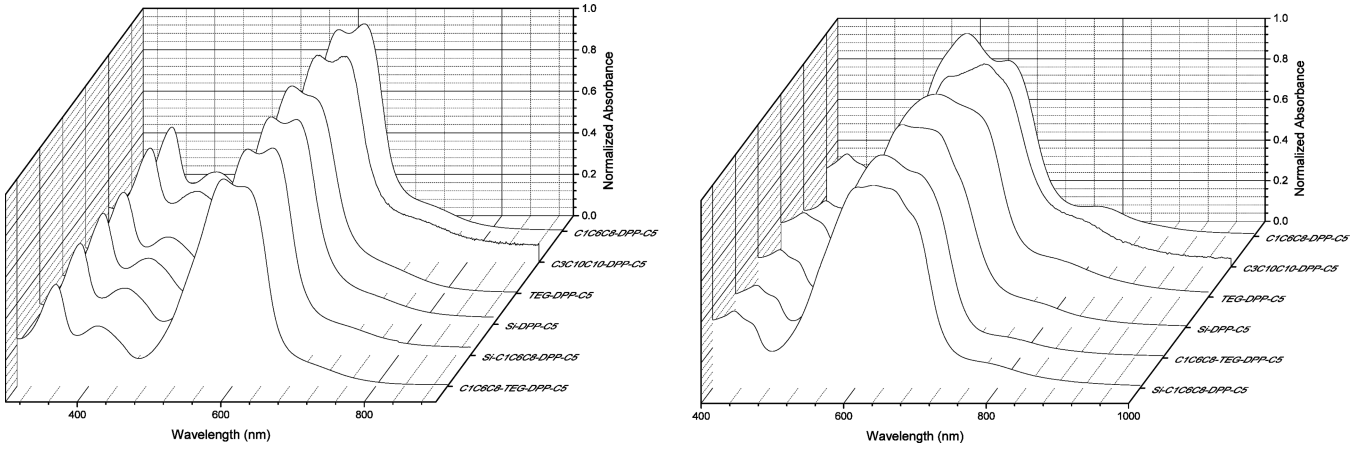

Figure 1. UV−vis−NIR absorbance spectra of the matrix polymers in dilute chloroform solutions (left) and as thin films (right).

RESULTS AND DISCUSSION

Monomer and Polymer Synthesis. The nomenclatures, structures, and synthesis of the DPP-based matrix polymers with different side chains are summarized in Scheme 1. The DPP monomers were synthesized from the thiophene-flanked DPP core and (mixtures of) side chain precursors under basic conditions,[17] followed by bromination with *N*-bromosuccinimide.[18−21] For DPP derivatives with siloxane-terminated side chains, alkene-terminated intermediates were reacted with 1,1,1,3,5,5,5-heptamethyltrisiloxane with the presence of Karstedt catalyst to give the desired products.[5] Detailed synthetic procedures of the monomers are provided in the Supporting Information.

The matrix polymers bearing various side chains were synthesized from Stille coupling polymerization based on the method previously reported.[8] The detailed procedure is provided in the Experimental Section. The pentamethylene group was chosen as the CBS owing to a good combination between charge-carrier mobility and processability based on our previous study.[15] After the polymerization was complete, the mixture was precipitated into methanol and purified with Soxhlet extractions with acetone, hexanes, and chloroform. The chloroform fraction was concentrated, and palladium residual was further removed with *N*,*N*-diethylphenylazothioformamide.[22] The products were obtained by precipitation into methanol followed by vacuum filtration, and were dried under high vacuum at 60 °C. The polymers were characterized by ^{1}H NMR, size-exclusive chromatography (SEC), UV−vis spectroscopy, ultraviolet photoelectron spectroscopy (UPS), thermal gravimetric analysis (TGA), and differential scanning calorimetry (DSC). The molecular weights of the polymers were measured with SEC with tetrahydrofuran as the eluent. The results are summarized in Table 1.

Optical Properties. The UV−vis−NIR spectra of the polymers in dilute chloroform solutions and as thin films are shown in Figure 1 and are summarized in Table 1. In chloroform solutions, all matrix polymers show similar dual-band absorbance spectra with maximum absorbance peaks at 590 and 625 nm, indicative of negligible influence of the side chains to the spectra in solution. These features in chloroform solutions are similar to the previously reported DPP-based CBS polymers and small molecules.[23] Compared to dilute solutions, all polymers in thin films show broader absorbance peaks occurring at longer wavelengths, which indicates the presence of J-aggregation of the chromophores. Surprisingly, such bathochromic shift is dependent on the side chain of the CBS polymer. For example, the absorbing peaks of C1C6C8-DPP-C5, which only contain alkyl side chains, exhibit a rather small red-shift of about 10 nm. As a comparison, the bathochromic shift of TEG-DPP-C5 is about 30 nm, which is the largest among all polymers. Similar behavior for TEG-containing polymers has been previously observed, which is attributed to the strong interactions between the highly polar side chains.[4,21,24] The extents of the bathochromic shifts of the other polymers are in the range between the alkyl-substituted and oligoether-substituted species.

Thermal Properties. The thermal stability of the polymers was confirmed by thermal gravimetric analysis (TGA). As presented in Figure S1 and Table 1, no decomposition is observed until around 400 °C for all polymers, indicating that side chains have little influence on thermal stability of the matrix polymers. The phase transition properties are evaluated

DOI: 10.1021/acs.macromol.7b01354
Macromolecules 2017, 50, 6202−6209

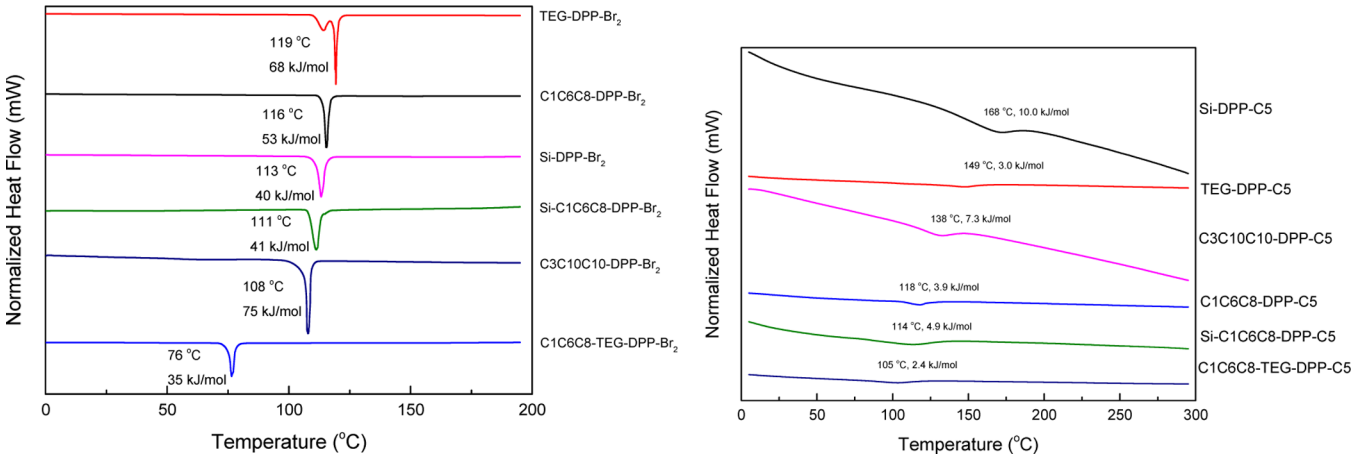

Figure 2. DSC thermograms of the monomers (left) and the matrix polymers (right). Data are normalized based on heats of fusion. Only the heating curves of the thermograms are presented.

Table 2. OFET Characteristics of the Pure CBS Polymers and Their *c*-SPBs with 5 wt % of C3C10C10-DPP-C0 as the Tie Chain Polymer

		pure polymers					*c*-SPBs with C3C10C10-DPP-C0[a] (5 wt %)				
		before annealing	after annealing				before annealing	after annealing			
polymer	annealing temp (°C)	μ_{avg} ($cm^2 V^{-1} s^{-1}$)	μ_{avg} ($cm^2 V^{-1} s^{-1}$)	μ_{max} ($cm^2 V^{-1} s^{-1}$)	V_{th} (V)	I_{on}/I_{off}	μ_{avg} ($cm^2 V^{-1} s^{-1}$)	μ_{avg} ($cm^2 V^{-1} s^{-1}$)	μ_{max} ($cm^2 V^{-1} s^{-1}$)	V_{th} (V)	I_{on}/I_{off}
C1C6C8-TEG-DPP-C5	80	1.9×10^{-4}	5.4×10^{-4}	1.2×10^{-3}	−2.8	$>10^3$	4.7×10^{-2}	7.6×10^{-2}	0.13	−6.7	$>10^5$
Si-C1C6C8-DPP-C5	80	6.5×10^{-4}	2.5×10^{-3}	3.3×10^{-3}	−5.2	$>10^4$	0.10	0.21	0.35	−7.4	$>10^5$
C1C6C8-DPP-C5	80	4.2×10^{-4}	2.3×10^{-3}	3.2×10^{-3}	−7.1	$>10^4$	0.20	0.28	0.36	−13	$>10^5$
C3C10C10-DPP-C5	120	5.4×10^{-4}	4.2×10^{-3}	6.5×10^{-3}	−5.2	$>10^4$	0.30	0.36	0.56	−10	$>10^5$
TEG-DPP-C5	120	7.8×10^{-5}	1.9×10^{-4}	2.1×10^{-4}	0.1	$>10^2$	1.8×10^{-3}	4.2×10^{-3}	5.3×10^{-3}	−13	$>10^3$
Si-DPP-C5	160	7.3×10^{-4}	2.8×10^{-3}	3.4×10^{-3}	−6.3	$>10^4$	0.11	0.26	0.38	−4.9	$>10^5$

[a]The average mobility of pure C3C10C10-DPP-C0 is 1.7 $cm^2 V^{-1} s^{-1}$.

by differential scanning calorimetry (DSC) for both monomers and polymers. The heating parts of the thermograms are shown in Figure 2, and the results for polymers are summarized in Table 1. The full graphs are provided in the Supporting Information. A strong influence from the side chains to the melting points and heats of fusion is observed for both monomers and polymers. As for monomers, symmetric side chains lead to higher melting points and heats of fusion. For example, TEG-DPP-Br_2 has the highest melting point (119 °C) among all monomers. C3C10C10-DPP-Br_2 exhibits the highest heat of fusion (75 kJ/mol). For C1C6C8-DPP-Br_2 and Si-DPP-Br_2, slightly higher melting points and lower heats of fusion compared to C3C10C10-DPP-Br_2 are observed, suggesting weaker intermolecular interactions. The asymmetric monomers, on the other hand, show lower melting points than the corresponding symmetric derivatives. The melting point (76 °C) and heat of fusion (35 kJ/mol) of C1C6C8-TEG-DPP-Br_2 are both lower than TEG-DPP-Br_2 and C1C6C8-DPP-Br_2. Similarly, the melting point of Si-C1C6C8-DPP-Br_2 is slightly lower than the symmetric C1C6C8-DPP-Br_2 and Si-DPP-Br_2, and the heat of fusion is similar to Si-DPP-Br_2.

The trend of thermal behaviors in polymers is generally similar to the monomers. Polymers with symmetric side chains tend to have higher melting points. For example, Si-DPP-C5 exhibits the highest melting point of 168 °C among all polymers, together with a heat of fusion as high as 10.9 kJ/mol. These high values suggest the strong interactions and high ordering of the polymer molecules owing to the presence of the siloxane-terminated side chains. C1C6C8-DPP-C5 has a melting point of 118 °C and heat of fusion of 4.0 kJ/mol. As a comparison, the melting transition of Si-C1C6C8-DPP-C5 occurs at 114 °C, which is lower than both Si-DPP-C5 and C1C6C8-DPP-C5, and the heat of fusion (4.7 kJ/mol) is in the range of the symmetric derivatives. In another series, C1C6C8-TEG-DPP-C5 exhibits a melting point of 104 °C and heat of fusion of 2.6 kJ/mol. These values are both lower than C1C6C8-DPP-C5 and TEG-DPP-C5 (149 °C, 2.8 kJ/mol) and are both the lowest in the series. The decrease in melting point and heat of fusion for the polymers with asymmetric side chains compared to the symmetric analogues proves the feasibility of our design, in which the break of symmetry disrupts the molecular packing drastically, leading to less energy required to destroy the intermolecular interactions. The correlation between the thermal behavior of the matrix polymers and the side chains provides us with a new strategy to design and produce semiconducting materials with improved processability.

Charge Transport Properties of Matrix Polymers and the Complementary Polymer Blends. To understand the influence of the side chains on the charge transport properties

DOI: 10.1021/acs.macromol.7b01354
Macromolecules 2017, 50, 6202−6209

of the matrix polymers and the *c*-SPBs with C3C10C10-DPP-C0 as the tie chain polymer, bottom-gate bottom-contact organic field-effect transistors (OFETs) were fabricated and measured. The specific processing methods for different materials are summarized in Experimental Section and Table S1. For *c*-SPB thin films, matrix polymers were premixed in solution with the tie chain polymer, C3C10C10-DPP-C0 (5 wt %), before fabrication. The devices were annealed at 80, 120, and 160 °C in a nitrogen-filled glovebox for desired durations before being tested in air. Average mobilities were calculated from more than 20 devices to obtain statistical meaningful results.

Typical p-channel charge transport behaviors are observed for all matrix polymers. Owing to the wide range of melting points of the matrix polymers, the devices were measured after annealed under different temperatures to optimize the best condition for each polymer. The results and optimized temperatures are summarized in Table 2. The mobility for each polymer annealed under different temperatures is shown in Table S1. Generally, higher mobilities are achieved under higher annealing temperatures, but the values drop a little with temperatures higher than the melting points. Take C1C6C8-DPP-C5 (mp 118 °C) as an example; devices annealed at 80 °C show higher average mobility (2.3×10^{-3} cm^2 V^{-1} s^{-1}) than ones annealed at 120 °C (1.4×10^{-3} cm^2 V^{-1} s^{-1}). As a comparison, for Si-DPP-C5 (mp 168 °C), a monotonous trend is observed for average mobilities with increasing annealing temperatures until 160 °C, and the mobility from 180 °C (2.0×10^{-3} cm^2 V^{-1} s^{-1}) is lower than that from 160 °C (2.8×10^{-3} cm^2 V^{-1} s^{-1}). Their typical output and transfer curves are shown in Figure S3. The polymers without oligoether side chains (C1C6C8-DPP-C5, C3C10C10-DPP-C5, Si-DPP-C5, and Si-C1C6C8-DPP-C5) exhibit similar average mobility in the range of 10^{-3} cm^2 V^{-1} s^{-1}, among which C3C10C10-DPP-C5 exhibits the highest mobility of 4.2×10^{-3} cm^2 V^{-1} s^{-1}. In general, the presence of TEG side chain leads to 1 order of magnitude decrease in the average mobility. The average mobility of C1C6C8-TEG-DPP-C5 is 5.4×10^{-4} cm^2 V^{-1} s^{-1}, almost 1 order of magnitude lower than the four polymers, and as for TEG-DPP-C5, the average mobility further decreased to 1.9×10^{-4} cm^2 V^{-1} s^{-1}. The poor performance of the TEG-containing polymers can be attributed to the lower degree of molecular ordering compared to other polymers,[24] which agrees with the GIXRD results discussed in the following section.

The charge transport properties of the *c*-SPBs with 5 wt % of the fully conjugated tie chain polymer, C3C10C10-DPP-C0, were further investigated. The typical output and transfer curves are shown in Figure S4. As shown in Table 2, for all polymers except for TEG-DPP-C5, the addition of the tie chain polymer leads to nearly 2 orders of magnitude improvement in charge carrier mobilities. For instance, the average mobility of *c*-SPB with C1C6C8-DPP-C5 reaches 0.28 cm^2 V^{-1} s^{-1}, which is more than 100 times higher than the pure matrix polymer. For C1C6C8-TEG-DPP-C5, the hole mobility of the *c*-SPB (7.6×10^{-2} cm^2 V^{-1} s^{-1}) is also higher than the pure polymer (5.4×10^{-4} cm^2 V^{-1} s^{-1}) by more than 2 orders of magnitude. As a comparison, for TEG-DPP-C5, the addition of the tie chain polymer only leads to approximately 1 order of magnitude higher than the pure matrix polymer.

These behaviors are similar to our previous results and consolidate the tie chain model.[14,15] According to this model, for the matrix polymers with alkyl spacers that break the conjugation along the polymer chain, interchain transport is the primary pathway for charge transport. The addition of the tie chain polymer leads to the formation of an interconnected network between crystalline π-aggregates and tie chain polymer and thus significantly improves charge transport. In addition, the smaller improvement of the *c*-SPB with TEG-DPP-C5 confirms the crucial role for the efficient interactions between the tie chain and the matrix polymers. In this blend, the highly polar TEG side chains from the matrix polymer and the nonpolar alkyl side chains from the tie chain polymer are incompatible with each other, leading to poor interactions between the polymers and less improvement in charge carrier mobilities compared to the other polymers. This model is further confirmed by the efficient charge transport of the *c*-SPB with C1C6C8-TEG-DPP-C5, which contains both nonpolar and polar side chains. In this case, the presence of the nonpolar side chains is sufficient to form good connections with the tie chain polymer, which allows for efficient charge transport within this blend. These results also agree with the GIXRD results, which will be further discussed in the following section.

Thin Film Morphology Characterization. To investigate the influence of the side chains on the morphologies of the polymer thin films so as to get a better understanding of the structure impact on electrical performance, tapping-mode atomic force microscopy (AFM) and grazing incidence X-ray diffraction (GIXRD) were used to probe the thin films of matrix polymers and their *c*-SPBs. The AFM images of the films before and after annealing are presented in Figures S5–S8. For all polymers except for TEG-DPP-C5 and C1C6C8-TEG-DPP-C5, slightly coarsened domains and larger grains are observed after annealing, indicating improved crystallinity upon annealing. For the TEG-containing polymers, on a contrary, the surfaces of the polymer thin films become softer after annealing at the specific temperatures. In general, the morphologies of polymers with different side chains have little difference between each other, suggesting a minor influence of the side chains to the morphology of the polymer thin films compared to the CBSs. As to the *c*-SPBs, no significant change of the surface morphologies could be observed compared to the pure polymers, which is not surprising considering the low concentration of the tie chain polymer (as low as 5 wt %) within the blends.

GIXRD was performed on the polymer thin films for more insight into the structure–property correlation of the matrix polymers and their corresponding *c*-SPBs. The samples for GIXRD measurement were annealed at temperatures indicated in Table 2 before testing. As is shown in Figures S9 and S10, all the samples, including the matrix polymers and their *c*-SPBs, show clear edge-on molecule packing mode with π–π stacking (0*k*0) peaks appearing in the in-plane direction and lamellar packing (*h*00) peaks in the out-of-plane direction. Particularly, the matrix polymer with the bulkiest alkyl side chains, C3C10C10-DPP-C5, shows the most orientated edge-on packing, which is in accordance with the highest charge carrier mobility among all polymers. On the contrary, the TEG-containing polymers show higher values of both in-plane and out-of-plane full width at half maximum (fwhm), which illustrates lower degrees of molecular ordering compared to other polymers. These results are in accordance with the poor electrical properties of these polymers. For all the matrix polymers except for C1C6C8-DPP-C5, the π–π stacking distances are around 3.7 Å, suggesting a minor influence of the side chain polarity to the π–π stacking distances. The larger

DOI: 10.1021/acs.macromol.7b01354
Macromolecules 2017, 50, 6202–6209

Table 3. Crystallographic Parameters for the Polymer and *c*-SPB Thin Films

	matrix polymers				blend with C3C10C10-C0 (5 wt %)			
materials	$\pi-\pi$ spacing (Å)	In-plane fwhm	lamellar spacing (Å)	out-of-plane fwhm	$\pi-\pi$ spacing (Å)	In-plane fwhm	lamellar spacing (Å)	out-of-plane fwhm
C1C6C8-TEG-DPP-C5	3.69	0.110	19.7	0.104	3.68	0.064	18.1	0.039
Si-C1C6C8-DPP-C5	3.69	0.081	23.3	0.059	3.67	0.096	23.1	0.075
C1C6C8-DPP-C5	3.78	0.111	15.1	0.048	3.76	0.195	14.9	0.093
C3C10C10-DPP-C5	3.69	0.075	22.8	0.046	3.68	0.074	22.5	0.045
TEG-DPP-C5	3.68	0.130	15.4	0.072	3.66	0.123	15.5	0.080
Si-DPP-C5	3.70	0.076	28.7	0.049	3.68	0.091	28.0	0.146

$\pi-\pi$ distance between C1C6C8-DPP-C5 molecules (3.78 Å) could be attributed to the steric hindrance caused by the close branching position of the side chains from the polymer backbone.[25,26] The lamellar packing distances of the six matrix polymers, however, are highly dependent on the side chains and vary in a wider range between 15.1 and 28.7 Å. For instance, comparing the two polymers with branched alkyl side chains, C1C6C8-DPP-C5 has a lamellar distance of 15.1 Å, which is significantly lower than C3C10C10-DPP-C5 (22.8 Å). This result is consistent with the fact that the length of the 2-hexyldecyl side chain within C1C6C8-DPP-C5 is shorter than the 4-decyltetradecyl groups to C3C10C10-DPP-C5.[25−27] Moreover, the lamellar packing distances of all asymmetric polymers are between their symmetric congeners.

For the *c*-SPBs, comparable but slightly shorter $\pi-\pi$ stacking distances are observed for all polymers. As is shown in Figure S10 and summarized in Table 3, the lamellar packing distances of *c*-SPBs are also slightly shorter than the corresponding matrix polymers except for TEG-DPP-C5. We also observe changes in the crystallinity of the polymers by adding the tie chain polymers. While the in-plane and out-of-plane fwhm of C3C10C10-DPP-C5 remains almost unchanged upon blending with the tie chain polymer, the fwhm values for the *c*-SPBs of all other matrix polymers are significantly different from the corresponding pure polymers. In general, if the side chains of the matrix are alkyl- and/or siloxane-terminated side chains, an increase in fwhm is observed. For example, the in-plane fwhm of Si-C1C6C8-DPP-C5 increases from 0.081 to 0.096 Å and the out-of-plane fwhm increases from 0.059 to 0.075 Å. On the contrary, for polymers with TEG side chains, nearly unchanged or decreasing fwhm values are observed. For TEG-DPP-C5, the in-plane fwhm decreases slightly from 0.130 to 0.123 Å, whereas the out-of-plane fwmh increases slightly from 0.072 to 0.080 Å. More interestingly, for C1C6C8-TEG-DPP-C5, both in-plane (0.110−0.064 Å) and out-of-plane (0.104−0.039 Å) fwmhs decrease drastically upon blending with C3C10C10-DPP-C0.

These phenomena can be attributed to the compatibility between the side chains of the matrix and the tie chain polymers. For the *c*-SPBs of polymers with TEG side chains (C1C6C8-TEG-DPP-C5 and TEG-DPP-C5), the incompatibility of the TEG side chains from the matrix polymers and the alkyl side chain from the tie chain polymer leads to segregation between the side chains. Consequently, the fwhm values of TEG-DPP-C5 remain almost unchanged, indicating that the tie chain polymer has marginal influence to TEG-DPP-C5. In the case of matrix polymers with nonpolar side chains (alkyl- and siloxane-terminated side chains), mixing between the side chains from the matrix and the tie chain polymers is expected due to increasing entropies, which leads to interrupted packing of the side chains between the matrix polymer molecules. Particularly, for C1C6C8-TEG-DPP-C5, the fwhm values in both directions decrease drastically, showing a much-improved crystallinity with the presence of the tie chain polymer. Similar segregation-induced crystallinity enhancement caused by incompatibility of the side chains has been previously reported for poly(3-alkylthiophene)s with alternating alkyl and semi-fluoroalkyl side chains, which forms highly ordered bilayer lamellar packing structure.[28] These results suggest poorer connections between the TEG-containing matrix polymers and the tie chain polymer and agree well with the OFET characterizations. We therefore conclude that such effect is the origin of the lower charge carrier mobilities of the *c*-SPBs with these polymers compared to other polymers. These results reveal that good compatibility and connection between the matrix and the tie chain polymers is highly crucial for efficient charge transport in *c*-SPBs.

CONCLUSION

In summary, we have synthesized six matrix polymers with various side chains and studied the influence of the side chains to the polymers and their *c*-SPBs. This study indicated that efficient interaction between the matrix and the tie chain polymer is crucial for charge transport in *c*-SPBs, which consolidates our design and model of the complementary semiconducting polymer blends. In addition, the novel design of polymer with asymmetric side chains also provides us with new strategy to build high-performance semiconducting materials with much improved processabilities. Currently, we are exploiting the high electronic performance and low melting point of Si-C1C6C8-DPP-C5 and pushing the material to the high limits by applying melt processing and alignment techniques.

EXPERIMENTAL SECTION

Materials and Characterizations. All reagents were purchased from Sigma-Aldrich and used without further purification unless otherwise noted. Anhydrous *N*,*N*-dimethylformamide is prepared from MB-SPS solvent purifying system. ^{1}H and ^{13}C NMR spectra were recorded on Varian Inova 300 or Bruker ARX 400 at 293 K with deuterized chlorofrom as solvent. Size exclusive chromatography (SEC) was performed in tetrahydrofuran under room temperature using a TOSOH Bioscience EcoSEC GPC system. The results were calculated based on the calibration curve generated from polystyrene standards. UV−vis−NIR spectra were measured with an Agilent Technologies Cary 6000i UV−vis−NIR spectrophotometer (300−1300 nm). All solution spectra were collected in chloroform and thin film spectra from drop-casted samples on glass substrate annealed at 120 °C for 10 min. Thermal gravimetric analyses (TGA) were carried out using a TA Instruments Q50. Samples were heated in platinum cells from 40 to 800 °C at a rate of 10 °C/min with the furnace (60 mL/min) and balance (40 mL/min) purged with nitrogen. Differential

DOI: 10.1021/acs.macromol.7b01354
Macromolecules 2017, 50, 6202−6209

scanning calorimetry (DSC) thermograms were measured using a TA Q5000 calorimeter calibrated with indium standard. Samples were sealed in hermetic aluminum pans. Measurements were performed with nitrogen as the purge gas (50 mL/min). The monomers were measured in one cycle from −40 to 200 °C. For the polymers, each measurement included two cycles from 0 to 300 °C. The heating and cooling rates for all measurements were 10 °C/min. Atomic force microscopy images were obtained on a Veeco Dimension 3100 AFM in tapping mode. Grazing incidence X-ray diffraction was performed at the Argonne National Laboratory on beamline 8-ID-E. Data were collected with a two-dimensional detector (Pilatus 1M) to obtain molecular packing information. The beam energy was 7.35 keV. Experiments were carried under ambient condition. One scan was carried for each sample with incident angle set at 0.2°.

General Method for Polymerization. 1,5-Bis((5-trimethylstannyl)thiophen-2-yl)pentane (88 μmol) and DPP monomers (88 μmol) were charged in a 35 mL microwave vessel. The monomers were dissolved in 15 mL of anhydrous toluene, and the solution was degassed with nitrogen for 15 min. $Pd_2(dba)_3$ (2.5 mol %) and tris(*o*-tolyl)phosphine (4 mol %) were quickly added to the solution under nitrogen. The vessel was sealed with a snap cap and transferred to a CEM Discover automatic microwave reactor. The reaction conditions were listed as follows: power cycling mode; power, 300 W; power cycles, 100; temperature, 150−180 °C; heating, 120 s; cooling, 30 s; pressure, 150 psi; stirring, high. Upon completion of the polymerization, the mixture was precipitated into methanol, and the solids were collected by a high quality glass thimble. The polymers were purified by Soxhlet extractions with acetone, hexane, and chloroform. The chloroform fraction was concentrated, and palladium was further removed with *N*,*N*-diethylphenylazothioformamide at 50 °C for 30 min.[22] The products were collected from precipitating into methanol followed by vacuum filtration and dried at 60 °C under high vacuum.

Fabrication of OFET Devices. A heavily n-doped Si wafer with a 300 nm SiO_2 surface layer (capacitance of 11 nF/cm^2) was employed as the substrate with Si wafer serving as the gate electrode and SiO_2 as the dielectric. The gold S/D electrodes were sputtered and patterned by photolithography technique. The device channel width was 1000 μm; the channel length was 5 μm for OFETs based on matrix polymer and 100 μm for OFETs based on blends. For the octadecyltrichlorosilane (OTS) modification, the silicon wafer (with Au bottom contact) was first cleaned with hot piranha solution (H_2SO_4 (98%):H_2O_2 (30% water solution) = 7:3). It was then further subjected to sonication sequentially in water and acetone for 5 min each. After dried in an oven, the silicon wafer was then put in a Petri dish with a small drop of OTS in the center. The dish was then covered and heated in a vacuum oven at 120 °C for 3 h, resulting in the formation of an OTS self-assembled monolayer on the surface. The OTS-modified substrates were rinsed successively with hexane, ethanol, and chloroform and dried by nitrogen. The semiconductor layer was deposited on the OTS-treated Si/SiO_2 substrates by spin-coating with speed of 1500/2000 rpm for 30 s. Polymer solutions were prepared in chloroform, and the concentrations were 5 mg/mL for Si-DPP-C5 and TEG-DPP-C5 and 10 mg/mL for the others. The devices were annealed in a N_2 glovebox under the specific temperature indicated in Table 2 and then tested in open air.

Device Characterization. Device characterization of the fabricated OFETs was carried out using a Keithley 4200 in ambient air. The field-effect mobility was calculated in the saturation regime by using the equation $I_{DS} = (\mu WC_i/2L)(V_G - V_T)^2$, where I_{DS} is the drain-source current, μ is the field-effect mobility, W is the channel width, L is the channel length, C_i is the capacitance per unit area of the gate dielectric layer, V_G is the gate voltage, and V_T is the threshold voltage.

■ ASSOCIATED CONTENT

Supporting Information

The Supporting Information is available free of charge on the ACS Publications website at DOI: 10.1021/acs.macromol.7b01354.

NMR, TGA, DSC curves, AFM figures, GIXRD images, OFET characteristics (PDF)

■ AUTHOR INFORMATION

Corresponding Author

*E-mail jgmei@purdue.edu (J.M.).

ORCID

Ying Diao: 0000-0002-8984-0051

Jianguo Mei: 0000-0002-5743-2715

Author Contributions

X.Z. and G.X. made equal contributions to the work.

Notes

The authors declare no competing financial interest.

■ ACKNOWLEDGMENTS

The authors acknowledge the financial support from the Office of Naval Research Young Investigator Program (ONR YIP), award N00014-16-1-2551 (Program manager: Paul Armistead), and MOE Key Laboratory of Macromolecular Synthesis and Functionalization, Zhejiang University (2016MSF003). Y.D. and G.Q. gratefully acknowledge partial support by National Science Foundation, Division of Materials Research under grant #1641854. This research used resources of the Advanced Photon Source, a U.S. Department of Energy (DOE) Office of Science User Facility operated for the DOE Office of Science by Argonne National Laboratory under Contract DE-AC02-06CH11357.

■ REFERENCES

(1) Mei, J.; Bao, Z. Side Chain Engineering in Solution-Processable Conjugated Polymers. *Chem. Mater.* **2014**, *26*, 604−615.

(2) Lei, T.; Wang, J.-Y.; Pei, J. Roles of Flexible Chains in Organic Semiconducting Materials. *Chem. Mater.* **2014**, *26*, 594−603.

(3) Feng, X.; Marcon, V.; Pisula, W.; Hansen, M. R.; Kirkpatrick, J.; Grozema, F.; Andrienko, D.; Kremer, K.; Mullen, K. Towards High Charge-Carrier Mobilities by Rational Design of the Shape and Periphery of Discotics. *Nat. Mater.* **2009**, *8*, 421−426.

(4) Kanimozhi, C.; Yaacobi-Gross, N.; Chou, K. W.; Amassian, A.; Anthopoulos, T. D.; Patil, S. Diketopyrrolopyrrole-Diketopyrrolopyrrole-Based Conjugated Copolymer for High-Mobility Organic Field-Effect Transistors. *J. Am. Chem. Soc.* **2012**, *134*, 16532−16535.

(5) Mei, J.; Kim, D. H.; Ayzner, A. L.; Toney, M. F.; Bao, Z. Siloxane-Terminated Solubilizing Side Chains: Bringing Conjugated Polymer Backbones Closer and Boosting Hole Mobilities in Thin-Film Transistors. *J. Am. Chem. Soc.* **2011**, *133*, 20130−20133.

(6) Sondergaard, R.; Hosel, M.; Angmo, D.; Larsen-Olsen, T. T.; Krebs, F. C. Roll-to-Roll Fabrication of Polymer Solar Cells. *Mater. Today* **2012**, *15*, 36−49.

(7) Xue, G.; Fan, C.; Wu, J.; Liu, S.; Liu, Y.; Chen, H.; Xin, H. L.; Li, H. Ambipolar Charge Transport of TIPS-Pentacene Single-Crystals Grown from Non-Polar Solvents. *Mater. Horiz.* **2015**, *2*, 344−349.

(8) Zhao, Y.; Zhao, X.; Zang, Y.; Di, C.-A.; Diao, Y.; Mei, J. Conjugation-Break Spacers in Semiconducting Polymers: Impact on Polymer Processability and Charge Transport Properties. *Macromolecules* **2015**, *48*, 2048−2053.

(9) Zhu, X.; Traub, M. C.; Vanden Bout, D. A.; Plunkett, K. N. Well-Defined Alternating Copolymers of Oligo(phenylenevinylene)s and Flexible Chains. *Macromolecules* **2012**, *45*, 5051−5057.

DOI: 10.1021/acs.macromol.7b01354
Macromolecules 2017, 50, 6202−6209

(10) Liang, Y.; Chen, Z.; Jing, Y.; Rong, Y.; Facchetti, A.; Yao, Y. Heavily n-Dopable π-Conjugated Redox Polymers with Ultrafast Energy Storage Capability. *J. Am. Chem. Soc.* **2015**, *137*, 4956−4959.
(11) Gasperini, A.; Bivaud, S.; Sivula, K. Controlling Conjugated Polymer Morphology and Charge Carrier Transport with a Flexible-Linker Approach. *Chem. Sci.* **2014**, *5*, 4922−4927.
(12) Schroeder, B. C.; Chiu, Y.-C.; Gu, X.; Zhou, Y.; Xu, J.; Lopez, J.; Lu, C.; Toney, M. F.; Bao, Z. Non-Conjugated Flexible Linkers in Semiconducting Polymers: A Pathway to Improved Processability without Compromising Device Performance. *Adv. Electron. Mater.* **2016**, *2*, 1600104.
(13) Erdmann, T.; Fabiano, S.; Milián-Medina, B.; Hanifi, D.; Chen, Z.; Berggren, M.; Gierschner, J.; Salleo, A.; Kiriy, A.; Voit, B.; Facchetti, A. Naphthalenediimide Polymers with Finely Tuned in-Chain π-Conjugation: Electronic Structure, Film Microstructure, and Charge Transport Properties. *Adv. Mater.* **2016**, *28*, 9169.
(14) Zhao, Y.; Zhao, X.; Roders, M.; Qu, G.; Diao, Y.; Ayzner, A. L.; Mei, J. Complementary Semiconducting Polymer Blends for Efficient Charge Transport. *Chem. Mater.* **2015**, *27*, 7164−7170.
(15) Zhao, X.; Zhao, Y.; Ge, Q.; Butrouna, K.; Diao, Y.; Graham, K. R.; Mei, J. Complementary Semiconducting Polymer Blends: The Influence of Conjugation-Break Spacer Length in Matrix Polymers. *Macromolecules* **2016**, *49*, 2601−2608.
(16) Zhao, Y.; Zhao, X.; Roders, M.; Gumyusenge, A.; Ayzner, A. L.; Mei, J. Melt-Processing of Complementary Semiconducting Polymer Blends for High Performance Organic Transistors. *Adv. Mater.* **2017**, *29*, 1605056.
(17) Rochat, A. C.; Cassar, L.; Iqbal, A. 1,4-Dioxopyrrolo[3,4-c]pyrroles. EP0094911A2, 1983.
(18) Tamayo, A. B.; Tantiwiwat, M.; Walker, B.; Nguyen, T. Q. Design, Synthesis, and Self-Assembly of Oligothiophene Derivatives with a Diketopyrrolopyrrole Core. *J. Phys. Chem. C* **2008**, *112*, 15543−15552.
(19) Li, Y.; Sun, B.; Sonar, P.; Singh, S. P. Solution Processable Poly(2,5-dialkyl-2,5-dihydro-3,6-di-2-thienyl-pyrrolo[3,4-c]pyrrole-1,4-dione) for Ambipolar Organic Thin Film Transistors. *Org. Electron.* **2012**, *13*, 1606−1613.
(20) Li, Y.; Singh, S. P.; Sonar, P. A High Mobility P-Type DPP-Thieno[3,2-b]thiophene Copolymer for Organic Thin-Film Transistors. *Adv. Mater.* **2010**, *22*, 4862−4866.
(21) Kanimozhi, C.; Yaacobi-Gross, N.; Burnett, E. K.; Briseno, A. L.; Anthopoulos, T. D.; Salzner, U.; Patil, S. Use of Side-Chain for Rational Design of n-Type Diketopyrrolopyrrole-Based Conjugated Polymers: What Did We Find Out? *Phys. Chem. Chem. Phys.* **2014**, *16*, 17253−17265.
(22) Nielsen, K. T.; Bechgaard, K.; Krebs, F. C. Removal of Palladium Nanoparticles from Polymer Materials. *Macromolecules* **2005**, *38*, 658−659.
(23) Naik, M. A.; Venkatramaiah, N.; Kanimozhi, C.; Patil, S. Influence of Side-Chain on Structural Order and Photophysical Properties in Thiophene Based Diketopyrrolopyrroles: A Systematic Study. *J. Phys. Chem. C* **2012**, *116*, 26128−26137.
(24) Shao, M.; He, Y. J.; Hong, K. L.; Rouleau, C. M.; Geohegan, D. B.; Xiao, K. A Water-Soluble Polythiophene for Organic Field-Effect Transistors. *Polym. Chem.* **2013**, *4*, 5270−5274.
(25) Lei, T.; Dou, J.-H.; Pei, J. Influence of Alkyl Chain Branching Positions on the Hole Mobilities of Polymer Thin-Film Transistors. *Adv. Mater.* **2012**, *24*, 6457−6461.
(26) Kang, I.; Yun, H. J.; Chung, D. S.; Kwon, S. K.; Kim, Y. H. Record High Hole Mobility in Polymer Semiconductors via Side-Chain Engineering. *J. Am. Chem. Soc.* **2013**, *135*, 14896−14899.
(27) Mei, J.; Wu, H.-C.; Diao, Y.; Appleton, A.; Wang, H.; Zhou, Y.; Lee, W.-Y.; Kurosawa, T.; Chen, W.-C.; Bao, Z. Effect of Spacer Length of Siloxane-Terminated Side Chains on Charge Transport in Isoindigo-Based Polymer Semiconductor Thin Films. *Adv. Funct. Mater.* **2015**, *25*, 3455−3462.
(28) Wang, B.; Watt, S.; Hong, M.; Domercq, B.; Sun, R.; Kippelen, B.; Collard, D. M. Synthesis, Properties, and Tunable Supramolecular Architecture of Regioregular Poly(3-alkylthiophene)s with Alternating Alkyl and Semifluoroalkyl Substituents. *Macromolecules* **2008**, *41*, 5156−5165.

DOI: 10.1021/acs.macromol.7b01354
Macromolecules 2017, 50, 6202−6209